

DOI 10.24425/ae.2024.148856

Electromagnetic processing of molten copper alloys in the induction furnace with cold crucible

ALBERT SMALCERZ¹  , LESZEK BLACHA¹ , JERZY BARGLIK¹ ,
IVO DOLEZEL² , TADEUSZ WIECZOREK¹ 

¹*Silesian University of Technology
Krasinskiego 8, 40-019 Katowice, Poland*

²*Faculty of Electrical Engineering, University of West Bohemia
Univerzitní 26, 301 00 Pilsen, Czech Republic*

e-mail: {[albert.smalcerz](mailto:albert.smalcerz@polsl.pl)/[leszek.blacha](mailto:leszek.blacha@polsl.pl)/[jerzy.barglik](mailto:jerzy.barglik@polsl.pl)/[tadeusz.wieczorek](mailto:tadeusz.wieczorek@polsl.pl)}@polsl.pl, idolezel@fel.zcu.cz

(Received: 19.06.2023, revised: 01.02.2024)

Abstract: Electromagnetic processing of molten copper is provided in a special kind of electrical furnace called an induction furnace with a cold crucible (IFCC), making it possible to successfully remove impurities from the workpiece. In order to analyze the process in a sufficient way not only electromagnetic, thermal and flow but also metallurgical and mass transfer phenomena in the coupled formulation should be taken into consideration. The paper points to an analysis of the kinetic process of lead evaporation from molten copper. It was shown that mass transport in the gas phase determines the rate of the analyzed evaporation process. The possibility of removal of lead from molten copper is analyzed and described.

Key words: furnace with cold crucible, induction melting, meniscus, purification of copper, vacuum refining

1. Introduction

Mathematical modeling of coupled electromagnetic, thermal, and flow phenomena in an IFCC is described in many papers, for instance in [1–7]. However, we still observe a lack of a more general approach to the problem. Melting of cast products in an IFCC offers various technological advantages, including higher purity of metals and their alloys. The use of a vacuum in the processing of liquid metals allows their degassing and, on the other hand, the removal of impurities with high vapor pressure from them. Providing such refining processes requires knowledge of not only electrothermal parameters. Of great importance are also physical and



© 2024. The Author(s). This is an open-access article distributed under the terms of the Creative Commons Attribution-NonCommercial-NoDerivatives License (CC BY-NC-ND 4.0, <https://creativecommons.org/licenses/by-nc-nd/4.0/>), which permits use, distribution, and reproduction in any medium, provided that the Article is properly cited, the use is non-commercial, and no modifications or adaptations are made.

chemical phenomena occurring during them in terms of thermodynamics and kinetics. The latter area concerns learning the mechanisms of mass transport both in the liquid metallic phase and in the gas phase. Obtaining such knowledge makes it possible to significantly influence a given technological process to increase its efficiency. The induction cold crucible melting and pouring of various materials became widely used in industry since the middle of the 90s. Different inter-metallic compounds, e.g. TiAl alloys that show excellent physical and chemical properties, are used as interesting construction materials, e.g. in automotive exhaust valves or turbine blades. The research presented in the paper makes it possible to analyze the possible application of an IFCC in a completely different metallurgical process for copper alloys and its comparison with a classical process provided in the vacuum induction crucible furnace.

The increase in demand for high-purity metals has contributed to the development of vacuum melting technologies. Vacuum metal refining technologies make it possible for both the evaporation of metallic bath impurities characterized by high vapor pressure and the release of gases dissolved in the bath. The rate of the evaporation process depends on many factors. The most important are the composition of the molten alloy, the process temperature, and the pressure in the melting system. Under reduced pressure conditions, the rate of the process in question may also be influenced by the mixing of the liquid alloy. In order to determine which of the mentioned factors determines the speed of the discussed process, it is necessary to conduct experimental research. The paper presents the results of research on the process of removing lead from liquid copper during its treatment in an induction furnace with a cold crucible. It should be noted that this technology is mainly used for melting titanium and its alloys, and the experiments discussed in the article indicate the desirability of using this technology for refining alloys of other metals.

2. Induction furnace with a cold crucible

Vacuum crucible induction furnaces are most commonly used for melting metal alloys and refining processes. A different technology is melting in induction furnaces with a cold crucible. Melting in such a unit involves placing the charge directly into a water-cooled inductor. This method has numerous advantages, including the ability to melt materials with high melting temperatures, the lack of interaction of the melt with the crucible lining, and the high purity of the final melting product. Disadvantages of this method include the difficulty of energy transfer at relatively low temperatures and difficulty in accurate power regulation mostly in a short period when the process begins but also during the full melting process.

In furnaces of this type, the water-cooled inductor is made of copper or aluminum. Typical values of the operating frequency of such units are several hundred kHz. A transistor generator of high-frequency current powers the circuit. The use of a series connection of capacitors and the use of an additional high-frequency transformer allows for increasing the voltage on the coil. A general disposition of the induction furnace with a cold crucible is shown in Fig. 1.

Figure 1 shows the ingot of Cu–Pb – the result of melting in IFCC.

The primary elements of the IFCC design, which are of great importance for computational modeling, especially near the contact zone of high-temperature melt with the cooled crucible, are presented in the scheme of the IFCC in Fig. 1: the cold crucible – 2 is the basic element of the design which distinguishes the IFCC from other types of induction furnaces or magnetohydrodynamic

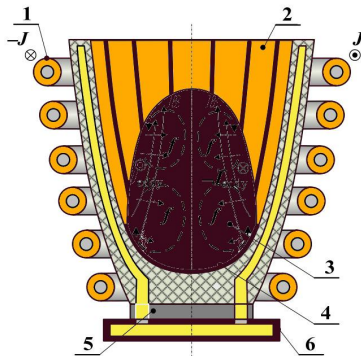


Fig. 1. IFCC furnace: 1 – inductor 2 – water cooled crucible, 3 – liquid copper, 4 – solid skull, 5 – ceramics, 6 – container

devices (MHDs) applied in metallurgy. The peculiarities of the IFCC design are the following: the crucible is made from material with high electrical conductivity like copper; it is segmented, i.e. divided into vertical, electrically insulated from each other sections. Each section has its own channel for water cooling; the crucible may have a water-cooled bottom as well. The characteristics of the melt are similar to those in any Vacuum Induction Melting (VIM) system. For numerical analysis it is necessary to take into consideration temperature dependent material properties like: – electrical conductivity, viscosity, thermal conductivity and others. The turbulent melt flow is determined by electromagnetic forces, which are the result of the interaction between eddy currents in a segmented conductive crucible and the magnetic field produced by the inductor. The scheme shows that due to the radial edges of each crucible section eddy currents are concentrated along the height of the melt. As for VIM, the buoyancy, the Marangoni forces connected with the mass transfer along an interface because of surface tension and electromagnetic forces' influence on flow melt, flow in a similar way.

The inductor is built as a single-phase or multi-phase system of coils, which is the source of an alternating electromagnetic field. The skull is a thin coagulated layer of fine-grained or porous solidified melt at the intensively cooled wall of the crucible. The skull makes it possible to reach high purity of high-temperature melt. Other elements of the IFCC design may be accordingly considered, if necessary, for electromagnetic and thermal modeling.

The analyzed process of lead evaporation from liquid copper is complex due to its heterogeneous nature. Its character depends not only on temperature and pressure in the melting aggregate but also on its type. This process has already been reported in many papers dealing with copper refining carried out in induction crucible vacuum furnaces [8–13]. However, there are no data on the rate of such a process realized in furnaces with a cold crucible. The original results obtained during the experiments provided in the vacuum IFCC furnace are presented in the paper.

3. Removal of lead from copper in IFCC furnace

3.1. Materials used in the study

Two kinds of scrap copper alloys were tested. The composition of them is shown in Table 1.

Table 1. Chemical composition

Alloy	Components %mas.								
	Pb	Sn	Al	Fe	Mn	Ni	Si	P	Cu
CuPb8	8	10	< 0.02	< 0.2	< 0.2	< 0.2	< 0.02	< 0.05	residue
CuPb1.9	1.9	12	< 0.01	< 0.2	< 0.2	< 2	< 0.01	< 0.4	residue

3.2. Test apparatus

The research is provided at the laboratory stand equipped with the ICCF vacuum furnace produced by the SECO-WARWICK company. Some important parameters of the stand are depicted in Table 2, while its general diagram is shown in Fig. 2(a).

Table 2. Technical and design parameters of the vacuum furnace used in the study

Parameters	IFCC furnace
Maximum active power	200 kW
Maximum vacuum	0.001 Pa
Temperature	2 073 K
Volume of crucible	1 dm ³

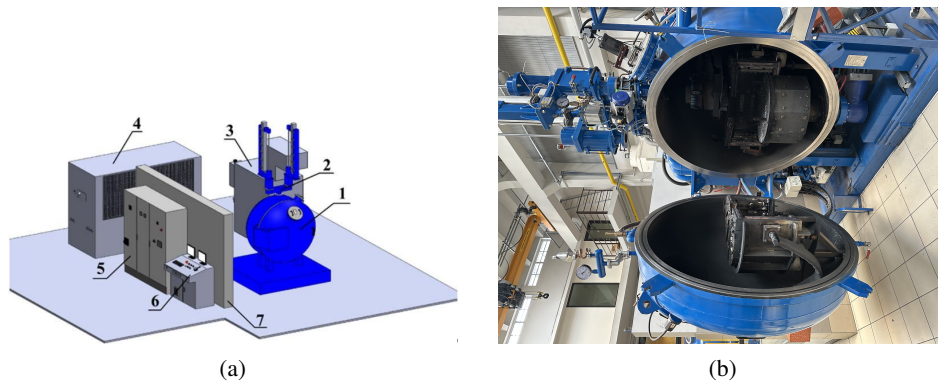


Fig. 2. Schematic diagram of the laboratory stand with ICCF furnace: 1 – vacuum chamber, 2 – sampling and temperature measurement airlock, 3 – generator, 4 – cooling system, 5 – control cabinet, 6 – operator panel, 7 – implosion wall (a); view of laboratory stand with VIM ISM 2-200 furnace (b)

3.3. Methodology and test parameters

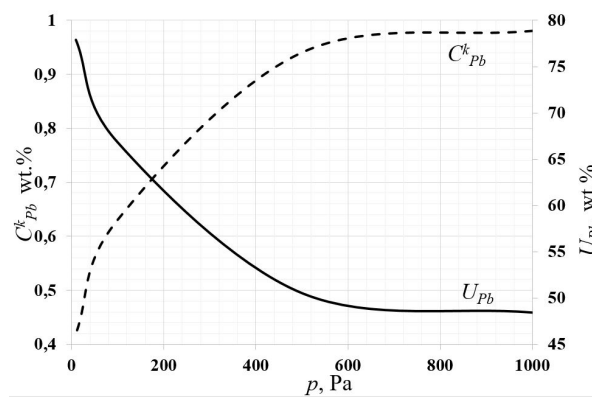
A sample of the test alloy of the appropriate mass (3 200–3 500 g) was placed in a water-cooled copper crucible. Implementation of all the experiments presented in the paper followed the fixed scheme. In the first stage, after placing the sample in the furnace, the pressure in the working chamber of the furnace was lowered, then heating was started and the charge was melted. After reaching the final temperature of the liquid metal, it was kept in the furnace for a specified period. The temperature was measured using a PtRh30-PtRh6 type thermoelectric sensor and an optical pyrometer. During the process, samples of liquid metal were taken, and its chemical composition was analyzed. For this purpose, the method of atomic absorption spectrometry was used, by means of the ASA Solar device. Experiments were provided at a temperature of 1 273–1 323 K and an active power of 180 kW. The operating pressure varied from 10 Pa to 1 000 Pa.

3.4. Experiments

Table 3 summarizes the results of experimental remelting of the tested copper alloys. It shows operational parameters (temperature, power, pressure), final lead content (C_{Pb}^k , wt.%), and the relative mass loss of lead (U_{Pb}), (Fig. 3).

Table 3. Results of experiments [14]

Type of alloy	T , K	P , kW	p , Pa	C_{Pb}^k , wt.%	U_{Pb}
Cu–Pb1.9 (1.9 wt.%)	1328	180	1 000	0.98	48.42
			500	0.94	50.52
			100	0.63	66.84
			10	0.42	77.89
Cu–Pb8 (8 wt.%)	1273	180	1 000	1.02	87.25
			500	0.88	89.00
			100	0.71	91.12
			10	0.55	93.12



(a)

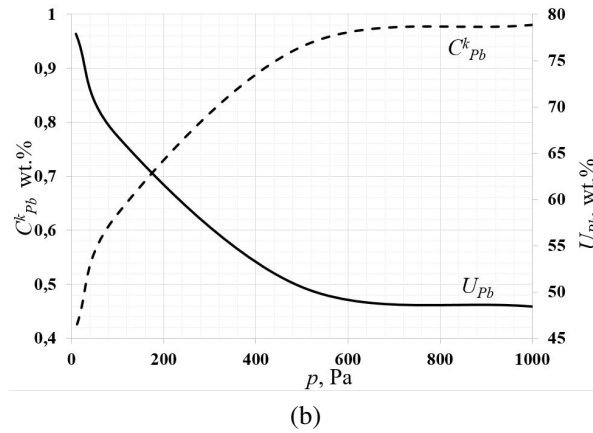


Fig. 3. Final lead content in the alloy and relative lead loss during melting of the alloys, at different working pressures: alloy Cu–Pb 1.9 (a); alloy Cu–Pb8 (b)

A distinct increase in the efficiency of removing lead from copper is observed; however, the working pressure in the furnace decreases. The final lead content in copper during the melting process of the alloy containing 8 wt.% lead was 0.55 wt.%, and for the alloy containing 1.9 wt.% lead was 0.42 wt.%. The relative mass loss of lead U_{Pb} with decreasing pressure from 1 000 Pa to 10 Pa increased for the lead-rich alloy from 87 to 93 wt. percent, and for the alloy with lower lead content from 48 to 78 wt. percent, respectively.

4. Kinetic analysis of the lead evaporation process

From a kinetic point of view, the analyzed lead evaporation process could be divided into three consecutive steps:

- transportation of lead from lower parts of melt to the surface,
- reaction of lead evaporation on the surface,
- transportation of lead vapor into the gas phase.

Formula (1) describes the overall mass transport coefficient of lead k_{Pb} .

$$\frac{1}{k_{Pb}} = \frac{1}{k^l} + \frac{1}{k^e} + \frac{1}{k^g}, \quad (1)$$

where: k^l is the mass transfer coefficient of lead in the liquid phase, k^g denotes the mass transfer coefficient of lead in the gas phase, and k^e stands for the evaporation rate coefficient of lead.

The evaporation process can generally be described by a first-order kinetic equation.

$$2.303 \log \frac{C_{Pb}^t}{C_{Pb}^0} = -k_{Pb} \frac{F}{V(t - t_0)}, \quad (2)$$

where: symbols c_{Pb}^0 and c_{Pb}^t denote the concentration of lead in copper at the beginning and after time t in wt. percentage, respectively, F denotes the evaporation area in m^2 , V stands for the volume of liquid copper in m^3 , and $(t - t_0)$ denotes the process duration in s .

Equation (2) may be used to determine the value of the coefficient k_{pb} taken from experimental data [14].

In the analyzed experiments, when temperature changes from 1 273 to 1 323 K, the estimated volume of liquid metal changes from $4.33 \cdot 10^{-4} \text{ m}^3$ to $4.38 \cdot 10^{-4}$. The density values of the studied alloys were determined based on the relations contained in [16].

When melting metals in induction furnaces, a convex meniscus on the surface of the liquid metal is observed [17, 18]. Figure 4 shows a picture at the surface of the investigated alloy during its melting in the ICCF furnace.

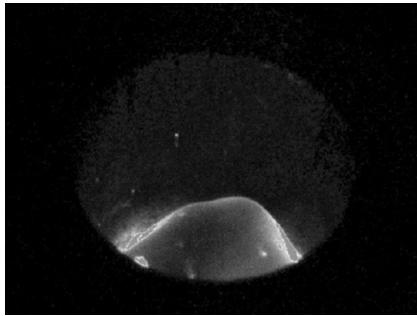


Fig. 4. Copper surface melted at ICCF furnace (active power of 170 kW)

In order to estimate the current surface area of the liquid Cu–Pb alloy, the method described in [19] is used. It consists of the following steps:

- Taking pictures of the molten copper with a high-speed camera (see Fig. 4),
- Determination of the geometry of the meniscus,
- Proposal of the curves describing the menisci for different parameters,
- Estimation of the area of the meniscus using specialized software (Wolfram Mathematica and MicroStation).

The estimated areas of liquid copper alloys in the discussed method varied from 227 to 230 cm^2 . In comparison, the total crucible cross-sectional area was 78.5 cm^2 . Table 4 summarizes the values of the overall lead transport coefficient k_{pb} for different process parameters, Fig. 5 shows the dependence of the overall lead transport coefficient on pressure.

Table 4. The overall mass transfer coefficients k_{pb} , k_{pb}^l , and k_{pb}^e

Type of alloy	T , K	p , Pa	k_{pb} , $\text{m}\cdot\text{s}^{-1}$	k_{pb}^l , $\text{m}\cdot\text{s}^{-1}$	k_{pb}^e , $\text{m}\cdot\text{s}^{-1}$
Cu–Pb1.9 (1.9 wt.%)	1 328	1 000	$1.71 \cdot 10^{-05}$	0.00014	0.000197
		500	$1.76 \cdot 10^{-05}$	0.00014	0.000197
		100	$1.81 \cdot 10^{-05}$	0.00014	0.000197
		10	$2.08 \cdot 10^{-05}$	0.00014	0.000197
Cu–Pb8 (8 wt.%)	1 273	1 000	$1.53 \cdot 10^{-05}$	0.000138	0.000102
		500	$1.60 \cdot 10^{-05}$	0.000138	0.000102
		100	$1.65 \cdot 10^{-05}$	0.000138	0.000102
		10	$1.81 \cdot 10^{-05}$	0.000138	0.000102

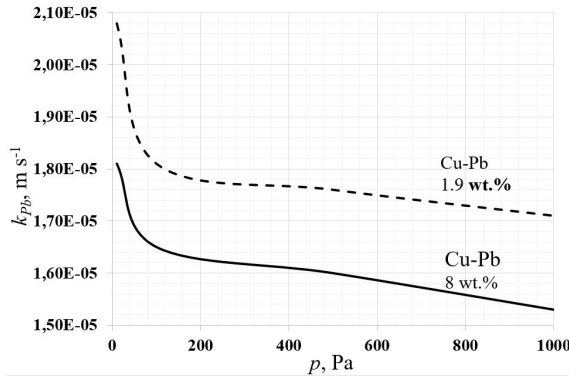


Fig. 5. Dependence of overall mass transfer coefficient on pressure

5. Mass transport in the liquid phase

In order to determine the lead transport coefficient k^l in the liquid phase for metals melted in induction furnaces, Machlin's relation [20] can be used. This relation can be written in the form:

$$k^l = \left(\frac{8D_{Pb}v_m}{\pi r_m} \right)^{0.5}, \quad (3)$$

where: v_m is the velocity of the liquid metal near the surface, r_m denotes the radius of the liquid metal at the surface (usually it could be taken as the inner radius of the crucible), and D_{Pb} stands for the diffusion coefficient of Pb in liquid copper.

Based upon (3) we observed that the coefficient k^l is proportional to the value of the velocity near the surface of the liquid metal. Machlin, based on his own observations, assumed that this velocity is practically independent of the electrical parameters of the furnace. For induction furnaces with a capacity of up to 1 Mg, its value is constant and equals $0.1 \text{ m}\cdot\text{s}^{-1}$. But in [21, 22] it was shown that this velocity depends also, among others, on the power of the furnace, the frequency of the inductor current, and the arrangement of the inductor-crucible system.

In the presented paper, in order to determine the k^l coefficient, we used values of the near-surface velocity [23], which were estimated for various alloys in experiments conducted in a vacuum induction furnace operating with similar electrical parameters. For liquid copper, the values of the velocity changed from $0.114 \text{ m}\cdot\text{s}^{-1}$ to $0.135 \text{ m}\cdot\text{s}^{-1}$. Table 4 summarizes the values of the mass transport coefficient k^l determined from relation (3). These values change from $1.38 \cdot 10^{-4} \text{ m}\cdot\text{s}^{-1}$ – $1.40 \cdot 10^{-4} \text{ m}\cdot\text{s}^{-1}$.

6. Evaporation process from the interfacial surface

In the analysis carried out, the relation in (4) was used to estimate the value of the rate constant k_{Pb}^e :

$$k_{Pb}^e = \frac{\alpha \cdot p_{Pb}^0 \cdot \gamma_{Pb} \cdot M_{Cu}}{(2\pi R \cdot T \cdot M_{Pb})^{0.5} \cdot \rho_{Cu}}, \quad (4)$$

where: α is the evaporation constant, p_{Pb}^0 denotes the equilibrium vapor pressure of lead over the liquid alloy in Pa, γ_{Pb} stands for the activity factor of lead in liquid copper, M_{Cu} and M_{Pb} represent the molar masses of copper and lead in $\text{g}\cdot\text{mol}^{-1}$, respectively, and ρ_{Cu} is the density of copper in $\text{g}\cdot\text{m}^{-3}$.

In order to determine the vapor pressure of lead over a liquid Cu–Pb alloy, data from the HSC thermodynamic database [24], as well as [25], were used. The k^e coefficients determined from relation (5) are summarized in Table 4.

In order to determine which of the above-discussed stages of the lead evaporation process determines its rate, the contributions of the resistance of both the mass transport process in the liquid phase (R^l) and the resistance associated with the reaction taking place on the surface of the liquid alloy (R^e) to the total resistance of the process were estimated by means of relations (5) and (6).

$$R^l = \frac{\left(\frac{1}{\beta^l}\right)}{\left(\frac{1}{k_{\text{Pb}}}\right)} \cdot 100\%, \quad (5)$$

$$R^e = \frac{\left(\frac{1}{k^e}\right)}{\left(\frac{1}{k_{\text{Pb}}}\right)} \cdot 100\%. \quad (6)$$

Figure 6 shows the change in the contributions of resistance R^l and R^e to the total resistance of the evaporation process as a function of the operating pressure prevailing in the ICCF furnace.

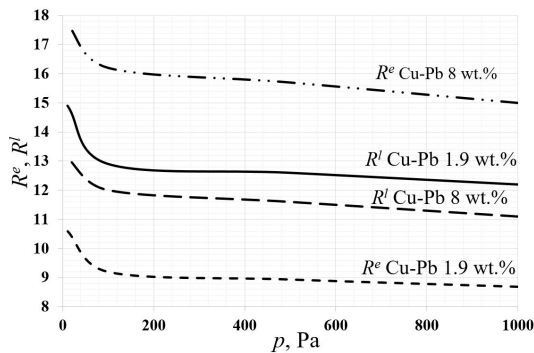


Fig. 6. Participation of resistance in liquid phase (R^l) and resistance of vaporization reaction (R^e) in overall resistance of lead evaporation from copper

Based upon the data presented in Fig. 6 we can state that for the temperatures and pressures used in the experiments, the lead evaporation process is determined mainly by mass transport in the gas phase. The share of mass transport resistance in the liquid metallic phase in the total resistance of the process does not exceed 15%. With decreasing pressure, there is a slight increase in the share of this resistance. At the same time, for all experiments, the share of resistance R^e in the total resistance of the process does not exceed 18%. The share of the total process resistance associated with the reaction, taking place on the surface of liquid copper R^e , and the resistance of mass transport in the liquid phase R^l in the total resistance of the lead evaporation process ranges from 21 to 31%.

7. Conclusions

Electromagnetic processing of high-quality materials in a vacuum induction furnace with a cold crucible makes it possible to achieve high purity of metals. One example of such an electromagnetic process dealing with lead evaporation from molten copper is described in the paper. The theoretical analysis of the process presented by the authors was verified by advanced experiments on a well-equipped laboratory stand, which allowed all important data to be identified and processed.

Based on the obtained results it was concluded that:

- The efficiency of the process of removing lead from copper increases as the working pressure in the furnace decreases.
- The final lead content in copper during the melting process of the alloy containing 8 wt.% lead was 0.55 wt.%, and for the alloy containing 1.9 wt.% lead was 0.42 wt.%.
- The relative mass loss of lead U_{Pb} increased with decreasing system pressure from 1 000 to 10 Pa for the alloy with 87 to 93 wt.%, for the alloy richer in lead, and for the alloy with lower lead content from 48 to 78 wt.%, respectively.

For all experiments in the assumed ranges of temperatures and working pressures in the melting unit, it was shown that the stage determining the speed of the lead evaporation process is mass transport in the gaseous phase.

- The maximum share of the mass transport resistance in the liquid metallic phase in the total resistance of the process does not exceed 15%. With a decrease in pressure, there is a slight increase in the share of this resistance.
- At the same time, for all experiments, the share of resistance R^e in the total resistance of the process did not exceed 18%.
- The share of the total resistance related to the course of the surface reaction with the reaction taking place on the surface R^e and the mass transport resistance in the liquid phase R^l in the total resistance of the analyzed evaporation process ranged from 21 to 31%.

Acknowledgments

The paper was prepared within a long term collaboration program between the Silesian University of Technology, Poland and the West Bohemia University, Czechia. The authors gratefully acknowledge the research funding provided by the Silesian University of Technology, grant number 11/040/BK_23/0029.

References

- [1] Hong Y., Li Y., Zhu D., Qie D., Wang R., Zhang S., *Multi-physics Numerical Investigation on the Mechanical Stirring in a Cold Crucible Melter*, Proceedings of the 23rd Pacific Basin Nuclear Conference, vol. 2, pp. 874–884 (2023), DOI: [10.1007/978-981-19-8780-9_84](https://doi.org/10.1007/978-981-19-8780-9_84).
- [2] Baake E., Nacke B., Bernier F., Vogt M., Mühlbauer A., Blum M., *Experimental and numerical investigations of the temperature field and melt flow in the induction furnace with cold crucible*, COMPEL – The international journal for computation and mathematics in electrical and electronic engineering, vol. 22, no. 1, pp. 88–97 (2003), DOI: [10.1108/03321640310452196](https://doi.org/10.1108/03321640310452196).
- [3] Skrigan I.N., Lopukh D.B., Vavilov A.V., Martynov A.P., *A Three-Dimensional Dynamic Model of Startup Heating during Induction Melting in a Cold Crucible*, Russian Electrical Engineering, vol. 92, pp. 150–153 (2021), DOI: [10.3103/S1068371221030123](https://doi.org/10.3103/S1068371221030123).

- [4] Umbrashko A., Baake E., Nacke B., Jakovics A., *Experimental investigations and numerical modelling of the melting process in the cold crucible*, COMPEL – The international journal for computation and mathematics in electrical and electronic engineering, vol. 24, no. 1, pp. 314–323 (2005), DOI: [10.1108/03321640510571336](https://doi.org/10.1108/03321640510571336).
- [5] Przyłucki R., Golał S., Buliński P., Smółka J., Palacz M., Siwiec G., Lipart J., Blacha L., *Analysis of the impact of modification of cold crucible design on the efficiency of the cold crucible induction furnace*, IOP Conference Series, VIII International Scientific Colloquium on Modelling for Materials Processing 21–22 September 2018, Riga, Latvia, vol. 355, no. 1 (2017), DOI: [10.22364/mmp2017.11](https://doi.org/10.22364/mmp2017.11).
- [6] Smalcerz A., Oleksiak B., Siwiec G., *The influence a crucible arrangement on the electrical efficiency of the cold crucible induction furnace*, Archives of Metallurgy and Materials, vol. 60, no. 3, pp. 1711–1715 (2015), DOI: [10.1515/amm-2015-0295](https://doi.org/10.1515/amm-2015-0295).
- [7] Pericleous K., Bojarevics V., Djambazov G., Harding R.A., Wickins M., *Experimental and numerical study of the cold crucible melting process*, Applied Mathematical Modelling 30, vol. 30, no. 11, pp. 1262–1280 (2006), DOI: [10.1016/j.apm.2006.03.003](https://doi.org/10.1016/j.apm.2006.03.003).
- [8] Ohno R., *Rates of evaporation of silver, lead, and bismuth from copper alloys in vacuum induction melting*, Metallurgical Transaction B, vol. 7, pp. 647–653 (1976).
- [9] Ozberk B., Guthrie R.I.L., *Evaluation of vacuum induction melting for copper refining*, Transactions of the Institution of Mining and Metallurgy, Section C, vol. 94, pp. 146–158 (1985).
- [10] Ozberk B., Guthrie R.I.L., *A kinetic model for the vacuum refining inductively stirred copper melts*, Metallurgical Transactions B, vol. 17, pp. 87–103 (1986), DOI: [10.1007/BF02670822](https://doi.org/10.1007/BF02670822).
- [11] Blacha L., *Bleientfernung aus Kupferlegierungen im Prozess der Vakuumraffination*, Archives of Materials and Metallurgy, vol. 48, no. 1, pp. 105–127 (2003).
- [12] Smalcerz A., Blacha L., *Removal of lead from blister copper by melting in the induction vacuum furnace*, Archives of Foundry Engineering, vol. 2020, no. 2, pp. 84–88 (2020), DOI: [10.24425/afe.2020.131307](https://doi.org/10.24425/afe.2020.131307).
- [13] Blacha L., Labaj J., Jodkowski M., Smalcerz A., *Research on the reduction of copper slag using an alternative coal range*, Metalurgija, vol. 59, no. 3, pp. 329–332 (2017).
- [14] Wecki B., *Analysis of the Influence of the Contact Area Size between the Liquid Metal Phase and the Gas Phase on the Efficiency of the Metal Refining Process in Induction Crucible Furnaces*, Ph.D. Thesis, Silesian University of Technology, Gliwice, Poland (2018).
- [15] Richardson F.D., *Physical chemistry of melts in metallurgy*, Academic Press London, pp. 483–493 (1974).
- [16] Evans R., Greenwood D., *Liquid metals*, Proceedings of the Third International Conference on Liquid Metals, 12–16 July 1976, Bristol, United Kingdom (1976).
- [17] Riemier B., Lange E., Hamayer K., *Investigation of the skull melting method for the generation of particulate material of inorganic compounds*, Archives of Electrical Engineering, vol. 60, no. 2, pp. 197–209 (2011), DOI: [10.2478/v10171-011-0019-2](https://doi.org/10.2478/v10171-011-0019-2).
- [18] Kudryash M., Behrens T., Nacke B., *Induction skull melting of oxides and glasses*, Archives of Electrical Engineering, vol. 54, no. 4, pp. 417–423 (2005), DOI: [10.22364/mhd.43.2.8](https://doi.org/10.22364/mhd.43.2.8).
- [19] Smalcerz A., Wecki B., Blacha L., *Influence of the power of various types of induction furnaces on the shape of the metal bath surface*, Advances in Science and Technology Research Journal, vol. 15, no. 3, pp. 34–42 (2021), DOI: [10.12913/22998624/138245](https://doi.org/10.12913/22998624/138245).
- [20] Machlin E.S., *Kinetics of vacuum induction refining—theory*, The American Institute of Mining, Metallurgical, and Petroleum Engineers (1961).
- [21] Przyłucki R., Golał S., Oleksiak B., Blacha L., *Influence of an induction furnace's electric parameters on mass transfer velocity in the liquid phase*, Metalurgija, vol. 1, pp. 67–70 (2012).

- [22] Blacha L., Przyłucki R., Gola S., Oleksiak B., *Influence of the geometry of the arrangement inductor – crucible to the velocity of the transport of mass in the liquid metallic phase mixed inductive*, Archives of Civil and Mechanical Engineering, vol. 11, no. 1, pp. 171–179 (2011), DOI: [10.1016/S1644-9665\(12\)60181-2](https://doi.org/10.1016/S1644-9665(12)60181-2).
- [23] Gola S., Przyłucki R., Barglik J., *Determination of a mass transfer area during metal melting in a vacuum induction furnace*, Archives of Materials and Metallurgy, vol. 59, no. 1, pp. 287–292 (2014), DOI: [10.2478/amm-2014-0047](https://doi.org/10.2478/amm-2014-0047).
- [24] Software Outokumpu HSC Chemistry® for Windows, ver. 6.1. Outokumpu Research Oy. Pori.
- [25] Plewa J., *Theory of metallurgical processes. Examples of calculations*, Publishing House of the Silesian University of Technology, Gliwice, Poland (1987).